Artificial neural network for random fatigue loading analysis including the effect of mean stress

J F Durodola*, S Ramachandra, S Gerguri and N A Fellows

Oxford Brookes University, Faculty of Technology, Design and Environment, Wheatley Campus, Oxford OX33 1HX, UK.

Abstract

The effect of mean stress is a significant factor in design for fatigue, especially under high cycle service conditions. The incorporation of mean stress effect in random loading fatigue problems using the frequency domain method is still a challenge. The problem is due to the fact that all cycle by cycle mean stress effects are aggregated during the Fourier transform process into a single zero frequency content. Artificial neural network (ANN) has great scope for non-linear generalization. This paper presents artificial neural network methods for including the effect of mean stress in the frequency domain approach for predicting fatigue damage. The materials considered in this work are metallic alloys. The results obtained present the ANN method as a viable approach to make fatigue damage predictions including the effect of mean stress. Greater resolution was obtained with the ANN method than with other available methods.

Keywords random fatigue, frequency, time domain, artificial neural networks, Dirlik, mean stress.

*Corresponding author, email: jdurodola@brookes.ac.uk; Tel: + 44 (0)1865 483501.

1. Introduction

The effect of mean stress is a significant factor in design for fatigue especially under high cycle service conditions. Various methods such as Goodman, Gerber and Soderberg, have been proposed for accounting for the effect of mean stress under predictable fatigue loading conditions [1]. The formulars relate the applicable stress amplitude to the mean stress and the strength of the material. Under random loading conditions, these methods are easily incorporated on a cycle by cycle basis in time domain cycle counting methods, especially using the rainflow counting method[1].

The incorporation of mean stress effect in random loading fatigue problems on a cycle by cycle basis is not yet achievable using current frequency domain spectral based methods. This problem is due to the fact that all cycle by cycle mean stress effects are zero frequency content which are all aggregated in the Fourier transform process into one content. The attempts to incorporate the effect of mean stress in frequency domain method have therefore focussed on using the global stress history mean value to account for this effect. Petrucci and Zucarrello [2] developed an empirical fit approach to incorporate the joined probability distribution effects of stress and mean stress using 45 loading signals. There has hardly been an independent rigorous verification of the results of using the method in the literature.

Dirlik's method is undoubtedly the most cited frequency domain solution for random fatigue problems. It did not however explicitly incorporate the effect of mean stress. The effect is implicitly present in the model because the spectral moments used, particularly zero spectral moment, incorporates the zero frequency content. Kihl and Sarkani [3] introduced a mean stress effect in a spectral based random fatigue analysis but this was limited to narrowband loading cases. Nieslony et al [4, 5] recently proposed a method which can be described as a power spectral transformation approach for including the effect of mean stress. This method is explained further in the section on theory. There have also not been an independent verification

of the procedure. There have been applications of ANN to other types of fatigue problems in the literature. Bhadeshia[6] indicated that fatigue is one of the most difficult mechanical properties to predict and suggested that the application of ANN could assist with establishing relationships between, material and loading variables, and crack propagation life. Artymiak et al[7] demonstrated the use ANN for the prediction of S – N curves based on a database of fatigue properties for steel alloys. Pujol and Pinto[8] used ANN to develop cumulative fatigue damage functions based on results of experiemental tests carried out on a steel alloy. Iacoviello et al [9] introduced ANN as a tool for the analysis of the effect of stress ratio on fatigue propagation in a duplex steel. In the realm of random loading fatigue, Kim et al [10] showed the possibility for ANN to be able to identify a spectral type and use this with various models such as Wirsching-Light[11], Zhao-Baker[12], Benasciutti-Tovo[13] and Dirlik[14] to predict fatigue damage.

This paper presents an alternative approach to those reviewed in the foregoing. Artificial neural networks have been known to provide greater scope for non-linear generalisation and have the ability to deal with a large number of input variables than direct application of optimisation methods [15], [16], [17]. The paper presents an artificial neural network frequency based approach for the analysis of random loading fatigue problems including the effect of mean stress. The materials considered in this work are metallic alloys. The method is based on the selection and use of input parameters that allow the artificial neural network to recognize signals and generalise for the solution of the problem. The input parameters include spectral moments, stress history – material properties. A broad range of spectral types, material properties, fatigue factor conditions and mean stress ranges were considered with up to 50,000 different signals. Effects of different input combinations and number of signals used for training were also considered.

2. Theory

In a previous publication [18], theoretical background covering aspects such as characterisation of random loading, fatigue life, type of loading, material properties, and artificial neural network method were highlighted. This paper summarises these aspects to provide a background and then adds essential details necessary to account for the effect of mean stress in machine learning frequency domain random fatigue loading analysis context.

2.1 Characterisation of random processes and fatigue loading

It is helpful because of a few subsequent steps that will be required to revisit the definition of the Fourier transform *X(f)* of a time domain signal *x(t),* which is given by equation (1). According to Parseval's theorem [19] the energy under the time and frequency domains are the same, as expressed in equation (2).

$$X(f) = \int_{-\infty}^{\infty} x(t)\, e^{2\pi i f t} dt \tag{1}$$

$$\int_{-\infty}^{\infty} |x(t)|^2 dt \quad = \quad \int_{-\infty}^{\infty} |X(f)|^2 df \tag{2}$$

where *t* represents time and *f* represents frequency. The linearity property of Fourier transform is expressed as in equation (3)

$$\mathcal{F}\{c_1 x_1(t) + c_2 x_2(t)\} = c_1 X_1(f) + c_2 X_2(f) \tag{3}$$

where $\mathcal{F}$ is a Fourier transform operator and c_1 and c_2 are constants that can be real or complex. The input output relationships of random processes are more conveniently described using the frequency domain representation. The power spectral density (PSD) equation (4) describes the variation of the power content of a signal e.g. S_x, in real terms with frequency.

$$G_x(f) = \lim_{T \to \infty} E\left[|X(f)|^2\right] \tag{4}$$

where $G_x(f)$ is the PSD and the symbol *E* is used to denote the expectation of the value in bracket. The value of $G_x(f)$ used in this work was normalised with respect to the sampling frequency. For the composite function in equation (3) and assuming that $c_1 = c$, $X_1 = X$ and $c_2 = 0$, the PSD can be written as shown in equation (5)

$$G_x(f) = c^2 \lim_{T \to \infty} E\left[|X(f)|^2\right] \tag{5}$$

In the context of fatigue, the power input during loading into a component is related to the fatigue damage by parameters based on the PSD. The main parameters used are the moments of the PSD which are given by equation (6) .

$$m_i = \int_0^\infty f^i G_x(f) df \tag{6}$$

where m_i is the *i* th moment of the PSD $G_x(f)$; $i = 0, 1, 2, 4$ are used for fatigue loading characterisation. Other parameters derived from the moments such as given in equations (7) and (8)

$$E(0) = \left(m_2 / m_0\right)^{1/2} \tag{7}$$

$$E(P) = \left(m_4 / m_2\right)^{1/2} \tag{8}$$

provide estimates for the number of upward mean crossing and the number of peaks in the signal per second respectively. The irregularity factor, γ, of the signal is given by equation (9)

$$\gamma = E(0) / E(P) = m_2 / \left(m_0 m_4\right)^{1/2} \tag{9}$$

reflects the spread of the process, γ tending to a value of 0 or 1 corresponds to a broad band or a narrow band signal respectively. An alternative description of bandwidth characteristics of a signal is given by the Vanmarcke's parameter [13] $q_x = [1 - m_1^2 / (m_0 m_2)]^{1/2}$

2.2 Frequency domain damage prediction models

The Miner's linear cumulative damage rule for different fatigue loading states (S_{ai}, S_{mi} *and* n_i) is given by equation (10)

$$E(D) = \sum_i n_i / N_i \tag{10}$$

where $E(D)$ is damage fraction, S_{ai}, S_{mi} and n_i, in the case of stress fatigue loading analysis, are the amplitude, the mean stress and number of cycles representing the loading corresponding to state *i*. N_i is the number of cycles under the loading state that on its own will cause fatigue failure. The life N_i is determined in terms of the fatigue properties of the material and the mean stress as highlighted in equations (11) and (12)

$$S_{ai} = \alpha_i \, a \, N_i^b \tag{11}$$

$$\alpha_i = (1 - S_{mi} / S_u) \tag{12}$$

where *a* and *b* are the fatigue strength and exponents values for the material based on stress amplitude. The parameter α_i in equation (10) is the Goodman's correction factor for accounting for the effect of mean stress and S_u is the ultimate strength of the material. Other empirical relations such as Soderberg, Morrow, Gerber, Smith Watson Topper relations are also used to account for the effect of mean stress [1]. The Goodman's relation which appears to have widespread usage is the basis of the approach used in this work. Instead of damage calculation based on the stress amplitude S_{ai}, an alternative route is to use the equivalent stress amplitude S_{a0} which from the Goodman's relation is given by equation (13)

$$\begin{aligned} S_{a0i} &= S_{ai} / \alpha_i = K.S_{ai} \\ K &= 1/(1 - S_{mi} / S_u) \end{aligned} \tag{13}$$

The frequency domain expression for fatigue damage prediction which includes Miner's rule [20] is generally written as in equation (14)

$$E(D) = E(P)\frac{T}{k}\int_0^\infty S^v p(S)dS \tag{14}$$

where T is the fatigue loading signal sampling time, $E(P) = (m_4 / m_2)^{1/2}$ is the number of peaks in the signal per second as indicated in equation (8), S is the stress range variable, $v = -1/b$ and $k = (2a)^{-1/b}$ and $p(S)$ is the probability distribution function expressing the possibility of the occurrence of S. Dirlik [14] in 1985 derived a probability distribution function $p(S)$ based on the combination of statistical Rayleigh and Normal distributions. The parameters of the distribution were determined using optimisation and heuristic observations to match the form of the distribution with results that were obtained using rainflow counting method for 70 different types of spectral. The form of the $p(S)$ obtained is given in equation (15)

$$p(S) = \left[\frac{D_1}{Q}e^{-Z/Q} + \frac{D_2 Z}{R^2}e^{-Z^2/2R^2} + D_3 Z e^{-Z^2/2}\right] / 2.m_o^{1/2} \tag{15}$$

where Z is the stress range normalised using the square root of the spectral moment m_0. All other parameters R, Q, D_1, D_2 and D_3 are intrinsically functions of the spectral moments m_i, $i=0,1,2$ and 4. This model does not explicitly contain the effect of mean stress and there are no parameters in the model such as ratios of mean stress to the ultimate or yield strength.

2.2.1 Mean stress effect in frequency domain fatigue analysis

A cycle by cycle mean stress parameter is not an available option in the frequency domain method as highlighted in the introduction. This is based on the fact that all mean stress effects are lumped together in the power spectral density as the zero frequency content.

Petrucci and Zuccarello [2] presented a fatigue damage formula in the form shown in equation (16).

$$E(D) = E(P)\,\exp[\psi(\alpha_x, \beta_x, v,\ \gamma_p)]/(2\pi k) \tag{16}$$

The function ψ, and its variables $\alpha_x, \beta_x, v,$ and γ_p are also functions of the spectral moments m_i, $i=0,1,2$ and 4 , the parameter $\gamma_p = S_{max}/S_u$ derived from the use of the Goodman's formula for accounting for the effect of mean stress. S_{max} is the maximum stress in the stress history, and k is a fatigue material property.

Nieslony et al recently presented a method for transforming a zero mean centre PSD to include the effect of mean stress. The transformed PSD could then be used with any spectral based probability distribution function such as the Dirlik's formula [14]. The presentation was based in the context of use of a transfer function [21]. The transformation could also be seen to result from the linearity of the Fourier transform method as highlighted in equation (3) and the PSD based on this as in equation (5). The approach may be summarised as follows. First the global mean stress of the spectrum loading, S_m, is determined. The global Goodman correction factor K_G is then given by equation (17)

$$K_G = 1/\left(1 - \frac{S_m}{S_u}\right) \tag{17}$$

The mean stress, S_m, is then subtracted from every data point in the S_x stress history to give $S_{xo} = S_x - S_m$, i.e thus shifting the spectrum to a global zero mean state. Denoting the G_{xo} as the power spectral density of the shifted signal S_{xo}, the modified power spectral density accounting for the effect of the mean stress as in equation (5) is given by $G_{xm} = K_G^2 G_{x0}$. This then is the function to be used in equation (4) in order to determine the moments m_{oi} , i =

0,1,2,4 to be used for the fatigue characterisation including the effect of mean stress. Nieslony also introduced other possible definitions of K_G .

This paper presents an artificial neural network frequency based approach which incorporates the effect of mean stress. As highlighted in the introduction, the method is based on the selection and use of input parameters that allows the artificial neural network to recognize signals and generalize for the solution of random loading fatigue problems that include the effect of mean stress. Various ANN models were developed and tested. Table 1 gives a summary of the inputs and output of the main ANN models considered. The additional parameters that were introduced as inputs during the development are given in equations (18) and following

$$\alpha_m = \left(1 - \frac{S_m}{S_u}\right) \quad \text{for } S_m > 0 \tag{18a}$$

$$\alpha_m = 1 \quad \text{for } S_m < 0 \tag{18b}$$

and $\alpha_c = {S_m}/{S_u}$; $\gamma_n = {S_{min}}/{S_u}$; where S_{min} is the minimum value of S_x; γ_p was previously introduced as part of the Petrucci Zuccarello's method description.

As to be expected the fatigue properties of the material and the spectral moments m_i, *i = 0,1,2,4* were essential inputs for fatigue analysis. The Goodman parameter α_m was also essential to account for the mean stress effect. Further exploration showed that the complementary parameter α_c improved the ability of the ANN to make predictions with greater accuracy and consistency. The parameters γ_p and γ_n were also found to be helpful in reducing the statistical spread of the predictions, in other words, they improved the precision of the prediction. The moments m_{oi}, *i = 0,1,2,4* and the K_G parameter were considered in order to implement the Nieslony's transformation approach [4] for the modification of Dirlik's formula [14]. Of course the Dirlik formula was not used in the ANN approach. The logarithmic value of the damage

E(D) was used as the output target value. This helped to reduce the impact of the spread of the damage values which was different by several orders. Data leading to damage values lower than 10^{-6} were rejected in order to avoid dilution of the training process with insignificant contributions to the training.

Although it has been suggested that half the sum of input and output neuron [22], [23] is adequate as the number to be set for the hidden layer neurons, experimentation with this number in this work did not show good prediction. The number of hidden layer neurons tested ranged from 10 to 80 and 20 was found to be adequate. The recommendation to use about 20 times the total number of neurons [23] provided some guidance for the number of signals constructed for the ANN training and testing in this study. In order to include extreme conditions, the numbers of signals developed and used ranged from 1000 to 50,000.

2.3 Machine learning artificial neural network implementation

As in previous work [18], three layers of neuron which is generally accepted as sufficient to represent any non-linear function approximation was used. Each of the hidden and output layer neuron is connected to the neurons in the preceding layer. The preceding layer to the output layer is the hidden layer and correspondingly the preceding layer to the hidden layer is the input layer. The strengths of the connections between neurons are described as weights.

Before an ANN can be used, it needs to be trained on data for which the inputs and the corresponding target outputs are known. The training process used in this work was based on the feedforward – backpropagation multilayer perceptron (MLP) method. The training proceeds by feeding known inputs into the network and obtaining its corresponding predictions for the output. In this process, each internal and output neuron receives a weighted sum of the input from the preceding neurons. The output from each neuron is transformed by an activation

function before being used as an input for the next layer of neurons. The sigmoid function which is numerically desirable in the perceptron model as it ensures that all values passing to the next neuron lie in the range [0,1] was used between the input and hiding layer. The parameters used in the ANN which consistently gave good prediction in a previous work can be found in reference [18]. The output layer used a linear transfer function, to ensure that erroneous outputs were easy to identify.

The output from the ANN will not in general match the known output corresponding to the inputs used from the data set, at least in the first feedforward through process. The mis-match error, usually the mean square error value, is then used in the backpropagation process to adjust or modify the weights so that better prediction can be made by the network in the next feedforward iteration process. A number of iterations of feedforward – backpropagation are required before the weights become useful and able to make a right prediction on the current data and subsequently on a previously unseen input data. Various backpropagation algorithms have been devised for the training of networks. One of the methods used in this analysis was based on the +Rprop algorithm which is known to have excellent convergence characteristics [15], [24]. The parameters required for the optimal convergence of the training in this approach has been identified for most problems and are not dependent on trial and error. For research flexibility purposes, the implementation of the ANN in this work was carried out using a set of in house routines developed in a MATLAB [25] environment. The Levenberg Marquart backpropagation method in MATLAB which generates equally good prediction as in the in-house programs but faster was later used.

2.4 Overall procedure

The description of the overall procedure used in this work is very similar to that presented with a flowchart in Durodola et al [18]. The analysis starts with the composition of trial space of

many different spectral forms as illustrated in Figure 1. Twelve different forms of spectra including those used by Dirlik, 1985 [14], Tovo [26] and Benasciutti and Tovo [13] as illustrated in Figure 1 were used in this study. The frequency values q_1, q_2, f_i , $i = 1,6$; spectral amplitudes d_i, $i=1,3$ and shape modification parameters d_4 and d_5 were chosen using the Latin Hypercube Sampling (LHS) [27] experimental design approach [28]. This facilitates maximum coverage of the fatigue loading space. The ranges of the material properties, i.e. the ultimate tensile strength, S_u, and fatigue strength and fatigue strength exponents a and b; and the limits of the spectral moment values m_i, $i = 0,1,2,4$ considered in the work are highlighted in Table 2.

As highlighted in the foregoing, different sample sizes ranging from 1000 to 50000 were analysed in the course of the study. The materials considered in this work are metallic alloys. Fatigue material properties S_u, a and b were sampled in the range 200 – 2000 MPa, (1.17 – 13.61) S_u and -0.0850 to -0.333 respectively. The range for the strength accommodates most alloys known from copper to maraging steels; both the fatigue slope b and strength coefficient a cover all typical or plausible values [2] which are dependent on factors such as size, surface finish, type of loading and notch factor.

For every combination of spectra parameters, the corresponding time domain signal for the selected spectrum was generated using equation (19) [29],

$$x_n(t) = \sum_{k=1}^{N} [2G_x(f_k)\Delta f]^{1/2} [\cos(2\pi f t + \phi_{k,n})] \tag{19}$$

where n is the sample number, N is the number of discretisation of the spectrum (PSD), with $f_k = (k - 0.5)\Delta f$ and $\phi_{k,n}$ are mutually independent random phase angles distributed uniformly over the range 0 to 2π. The maximum frequency considered for the fatigue data in the study was 200 Hz. The sampling frequency used varied from the corresponding Nyquist frequency of 400 Hz to 6.40 kHz. The higher sampling frequencies were considered in the light of recent findings [30]. Up to 5000 discretisation of the frequency range and 32000 time steps

were considered. In order to introduce a mean stress effect, the signal was then randomly shifted along the stress ordinate so that in general $S_m \neq 0$. The final *x(t)* obtained was then scaled so that the highest peak or deepest valley lied within 5 to 83% of the ultimate tensile strength value. The mean stress values incorporated ranged from -0.6 to 0.6S_u. This scaling reduced the possibility of any of the time data leading to extremely low values of oscillation before final fatigue damage occurs. This process provided a pool of input output for the training of the ANN described in section 2.3. The signals were analysed using ANN structures described in the foregoing as well as in house rainflow counting routine. The analysis used the material fatigue properties to determine corresponding damage intensity (i.e. damage per second) for each of the signals generated.

3. Results

This section presents the results obtained in the process of developing the ANN and demonstrates the levels of accuracy that was obtained in comparison with the use of the rainflow counting method directly to predict damage. The level of accuracy obtainable is first demonstrated and then comparison is made with the results of the Dirlik's method and Dirlik's method with transformed PSD [4]. The effects of varying the numbers of signals used in the training of the ANN are also highlighted. As in the previous work [18], several spectrum shapes and an extensive range of material property values were considered. It is helpful to highlight the three levels of process involved in generating the results obtained. These are called 'trial', 'batch' and 'signal' in the description of the analysis and results. 'Trial' was the highest level, a trial consisted of a batch or batches of tests, each batch contained a number of signals. A batch normally contained many signals and a trial consisted of many batches. The reason for these levels of analysis is to try to investigate the consistency of predictions from many independent studies. Consistency of results in the broad scope and instances of data demonstrates that the generalisation of the ANNs developed are statistically stable in terms of predictions.

3.1 ANN prediction of damage including effect of mean stress

The aim of this section is to demonstrate the agreement of the ANN prediction with rainflow counting method. The results shown here are based on an ANN4, see Table 1, developed using 50000 stress histories all generally including $S_m \neq 0$ states that were randomly effected. Two typical stress histories with different mean stress levels are shown in Figures 2(a) and (b). Figures 2(c) and d) show that the sampling used in the investigations covered narrow to broadband signals as well as values of the fatigue property *a* comprehensively. The value of *b* also cover the full range of -0.333 to -0.085 comprehenesively too. The development used 70, 15 and 15% proportions of the stress history population for training, validation and testing respectively. Figures 3 (a) – (d) show the correlation between the logarithmic values of damage predicted using ANN4 and rainflow counting results for training, validation, testing and all signals combined respectively. As can be seen in the results, a broad range of values of damage fraction between 10^{-25} and 1 was tested in each case. The inputs to the network included, the four spectral moments m_i, i = 0, 1, 2 and 4; three material properties *a, b* and S_u and four other parameters α_m, α_c, γ_n and γ_p. The output was the logarithm of the damage value E(D). The ANN developed on this bases was then used to analyse new set of cases generated data. One trial was used which contained two batches and each batch contained 500 signals or patterns. Miner's rule with rainflow counting was used to analyse the same stress histories and materials. Figures 4(a) and (b) show the plot of the results from both ANN and rainflow counting method for the two batches. The correlation and coefficient of fit displayed on the plots are 0.8544 and 0.9804; and 0.9923 and 0.9945 respectively. Tables 3(a) and (b) also show the comparison of the logarithmic value of the damage for 10 signals for each of the two batches for the ANN and the rainflow counting methods. The results can be seen in both the plots and tables to be quite close to the rainflow counting method results.

3.2 Comparison of prediction with other methods

This section compares the performance of the ANN4 prediction with Dirlik's method and Dirlik's method with the power spectral density modified by using the Goodman's relation. The Goodman's factor was based on global mean stress as highlighted in the foregoing. ANN4 was used to analyse freshly generated stress histories. Ten trials were carried out, with each containing ten batches of tests and each batch contained 500 signals or patterns. The ten trials and ten batches allowed 100 correlation tests to be carried out for the comparisons. This process led to the generation of 50,000 signals for testing that were independent of the original 50,000 that were used for training and validation of the neural network. The coefficient of fit between rainflow counting and predicted results were determined. Figures 5(a) to (c) gives plot of results for one random trial and batch. As can be seen in the plots the results from ANN, Dirlik and modified Dirlik showed good to excellent correlation and coefficients of fit with the rainflow counting method. The differences lied primarily in the scatter of the results which are described by the correlation and the coefficient of fit for each methods. Figures 6(a) to (c) give the probability and cumulative probability distribution plots for the coefficient of fits for all the 100 independent batches tested. The probability distribution plot for the coefficient of fit shows that the ANN values varied between 0.90 and 1.03. The corresponding values for the Dirlik and modified Dirlik were 0.74 and 1.11, and 0.97 and 1.19 respectively. The unmodified Dirlik method showed the greatest spread, followed by the modified Dirlik and ANN showing the lowest spread. Dirlik's method under predicts by 30% in some cases and over predicts by 11% in some cases. ANN under predicts by 10% in some cases and over predicts by 3% in some cases. Modified Dirlik under predicted by 3% in some cases and over predicts by 19%. The limits indicated here relate to the 10 trials used for this results. Further trials were carried out as indicated in section 3.3. As in the case of section 3.1, Tables 4(a) and (b) show the comparison of the logarithmic value of the damage for 10 signals for each of two batches of 500 signals or patterns using ANN4 and rainflow counting, Dirlik and modified Dirlik methods.

The results can be seen in the tables to be quite close to the rainflow counting method results especially for the ANN4. For numerical comparison purposes, Tables 5(a) and (b) give the coefficients of fit for two trials out of the 10 trials used in total, for the different damage prediction methods. The predictions are generally very good to excellent especially for the ANN4 method.

3.3 Effect of input characteristics

The effect of input parameters on the performance of prediction is analysed in this section. The input parameters are those characterising ANN1, ANN2, ANN3 and ANN5 having presented results for ANN4 in sections 3.1 and 3.2. Ten trials were carried for the analysis of each of the ANN method, each trial consisted of ten batches and each batch consisted of 500 signals as in the case of section 3.2. Also as in that case this process led to the generation of independent 50,000 signals for each of the methods tested. Figures 7 to 10 give the probability and cumulative probability distribution plots for the coefficient of fits for the 100 independent batches tested in each case. As can be seen in the plots, the unmodified Dirlik showed the most spread in the coefficient of fit for predictions. It can be seen that ANN1 which is based on minimal information of the mean stress effect showed good performance. There was progressive improvement in the results obtained as the number of inputs increased in ANN2 and ANN3. ANN5 which is based on the transformation of the spectral density also showed very good performance but appears to lead to occasionally unexpectedly high deviations. This trait also shows in the modified Dirlik method.

3.4 Effect of number of signals used for training the ANN

The trials in this case were based on the ANN4 network. The numbers of patterns used for the training of the network were 500, 1000, 2000, 5000, 10000, 20000 and 50000 as indicated in Table 5. As in section 3.1, 70, 15 and 15% proportion of the stress history population were used for training, validation and testing respectively for the development of the networks. The

networks were then tested using one trial each; each trial consisted of ten batches with each batch consisting of 500 signals or patterns. The mean coefficient of fit and the root mean square error for the ten batches for the different predictions methods are shown in Table 5(a). The mean values appear very good for all cases but values of the root mean square errors can be seen to be high for the low number of signal cases. The standard deviation of the coefficient of fit and of the root mean square error values shown in Table 5(b) also indicate the general improvement in trend with increasing number of signals used for training the network.

4. **Discussion**

Although ANN1 type performed excellently well for the cases of zero mean stress effect [18] there was no expectation for it to give good performance in the case that mean stress effect is present. Preliminary investigation with a large training data set 50000 with ANN1 showed direct correlation between prediction and rainflow counting results. The resolution was however the general issue. The difference between predicted and rainflow result derived from the coefficients of fit in some cases were as high 30%. ANN2 performed much better with possible percentage difference of about 11%. The plots in Figures 6 to 10 show that ANN4 was the most consistent in yielding a maximum difference of 10%. This led to the acceptance of the ANN4 as the best model. Although ANN5 based on modified spectral moments showed generally good performance, it was found to be susceptible to occasional significant difference between predicted and target values. This issue was also found with the modified Dirlik method.

One of the known issues that could happen in ANN modelling is the possibility of over fitting during learning. In this circumstance the ANN is able to give very accurate predictions with seen data but will be incapable of the same performance on unseen data. The problem is straight forward to detect. When new unseen data is used to test an ANN with over fitting learning defect, the prediction from the network will deviate significantly from expectation. As can been seen in section 3, several new independent trials with large population of signal of size 50000

in many cases were used in this work to verify the ANNs developed. No over fitting learning issues were detected.

The results from the number of signals used for training showed that 5000 data sets upwards gave about the same level of standard deviation in the coefficient of fit. It was also found that the performance convergence characteristics during training were more consistent when large data sets were used. From Figure 6, 90% of the ANN4 predictions lied between a factor of 94% and 101% of the rainflow counting target values. Also from the figure, it can be seen that 100% of the predictions was between 90% and 103% of the rainflow counting results. In the case of modified Dirlik an over prediction of 20 to 30% is possible. In general, the ANN approach developed herein provides a new viable avenue for random fatigue damage prediction even for the cases where mean stress effect is present.

It is helpful to highlight the limits of the analysis carried out in this paper. The spectral and material properties considered have been limited to those practically feasible values shown in Table 1. The limits can however be changed to cover any application that may be found to fall out of the existing scope. An ANN model is usually only used to solve similar problems as those used for its training.

5. Conclusions

Artificial neural network approach has been presented as a new viable spectral based method for the analysis of random fatigue loading problems including the effect of mean stress. Excellent correlation factors and coefficients of fit were obtained when compared to the rainflow counting method. The method yields better agreement and resolution with time domain results compared to recent frequency domain methods that include the effect of mean stress. The correction required for ANN4 to match rainflow counting is less than 6% with a probability confidence level of 90%. Existing methods can deviate by up to 33% from rainflow counting

results. Future work will be considering performance of ANNs on non Gaussian random fatigue loading signals.

List of Tables

List of Figures

References

1. Dowling, N.E., *Mechanical behavior of materials: engineering methods for deformation, fracture, and fatigue*. 2012: Pearson.
2. Petrucci, G. and B. Zuccarello, *Fatigue life prediction under wide band random loading.* Fatigue & Fracture of Engineering Materials & Structures, 2004. **27**(12): p. 1183-1195.
3. Kihl, D.P. and S. Sarkani, *Mean stress effects in fatigue of welded steel joints.* Probabilistic engineering mechanics, 1999. **14**(1): p. 97-104.
4. Niesłony, A. and M. Böhm, *Mean stress value in spectral method for the determination of fatigue life.* acta mechanica et automatica, 2012. **6**: p. 71-74.
5. Niesłony, A. and M. Böhm, *Mean stress effect correction using constant stress ratio S–N curves.* International journal of fatigue, 2013. **52**: p. 49-56.
6. HKDH, B., *Neural networks in materials science.* ISIJ international, 1999. **39**(10): p. 966-979.
7. Artymiak, P., et al., *Determination of S–N curves with the application of artificial neural networks.* Fatigue & Fracture of Engineering Materials & Structures, 1999. **22**(8): p. 723-728.
8. Pujol, J.C.F. and J.M.A. Pinto, *A neural network approach to fatigue life prediction.* International Journal of Fatigue, 2011. **33**(3): p. 313-322.
9. Iacoviello, F., D. Iacoviello, and M. Cavallini, *Analysis of stress ratio effects on fatigue propagation in a sintered duplex steel by experimentation and artificial neural network approaches.* International Journal of Fatigue, 2004. **26**(8): p. 819-828.
10. Kim, Y., H. Kim, and I.-G. Ahn, *A study on the fatigue damage model for Gaussian wideband process of two peaks by an artificial neural network.* Ocean Engineering, 2016. **111**: p. 310-322.
11. Wirsching, P.H. and M.C. Light, *Fatigue under wide band random stresses.* Journal of the Structural Division, 1980. **106**(7): p. 1593-1607.
12. Zhao, W. and M.J. Baker, *On the probability density function of rainflow stress range for stationary Gaussian processes.* International Journal of Fatigue, 1992. **14**(2): p. 121-135.
13. Benasciutti, D. and R. Tovo, *Spectral methods for lifetime prediction under wide-band stationary random processes.* International Journal of Fatigue, 2005. **27**(8): p. 867-877.
14. Dirlik, T., *Application of computers in fatigue analysis*. 1985, University of Warwick.
15. Farley, S.J., et al., *High resolution non-destructive evaluation of defects using artificial neural networks and wavelets.* Ndt & E International, 2012. **52**: p. 69-75.
16. Farley, S.J., et al., *A Neural Network Approach for Locating Multiple Defects*, in *Advances in Experimental Mechanics Vi*, J.M. DulieuBarton, J.D. Lord, and R.J. Greene, Editors. 2008. p. 125-131.
17. Hernandez-Gomez, L.H., et al., *Locating defects using dynamic strain analysis and artificial neural networks*, in *Advances in Experimental Mechanics IV*, J.M. DulieuBarton and S. Quinn, Editors. 2005. p. 325-330.
18. Durodola, J., et al., *A pattern recognition artificial neural network method for random fatigue loading life prediction.* International Journal of Fatigue, 2017. **99**: p. 55-67.
19. Newland, D., *An introduction to random vibrations, spectral and wavelet analysis. 1993.* Essex, England: Longman Scientific & Technical.

20. Bishop, N.W. and F. Sherratt, *Finite element based fatigue calculations*. 2000: NAFEMS.
21. Bendat, J.S. and A.G. Piersol, *Random data: analysis and measurement procedures*. Vol. 729. 2011: John Wiley & Sons.
22. Heaton, J., *Introduction to neural networks with Java*. 2008: Heaton Research, Inc.
23. www.statsoft.com. *Neural Networks*. July 2016 [cited 2016 July].
24. Igel, C. and M. Hüsken. *Improving the Rprop learning algorithm*. in *Proceedings of the second international ICSC symposium on neural computation (NC 2000)*. 2000. Citeseer.
25. The MathWorks Inc(2010), *MATLAB The language of technical computing*. 2010: USA.
26. Tovo, R., *Cycle distribution and fatigue damage under broad-band random loading.* International Journal of Fatigue, 2002. **24**(11): p. 1137-1147.
27. Mckay, M., R. Beckman, and W. Conover, *A Comparison of Three Methods for Selecting Values of Input Variables in the Analysis of Output from a Computer Code.* Technometrics, 2000: p. 55-61.
28. Montgomery, D.C., *Design and analysis of experiments*. 2008: John Wiley & Sons.
29. Shinozuka, M., *Monte Carlo solution of structural dynamics.* Computers & Structures, 1972. **2**(5-6): p. 855-874.
30. Quigley, J.P., Y.-L. Lee, and L. Wang, *Review and Assessment of Frequency-Based Fatigue Damage Models.* SAE International Journal of Materials and Manufacturing, 2016. **9**(2016-01-0369).

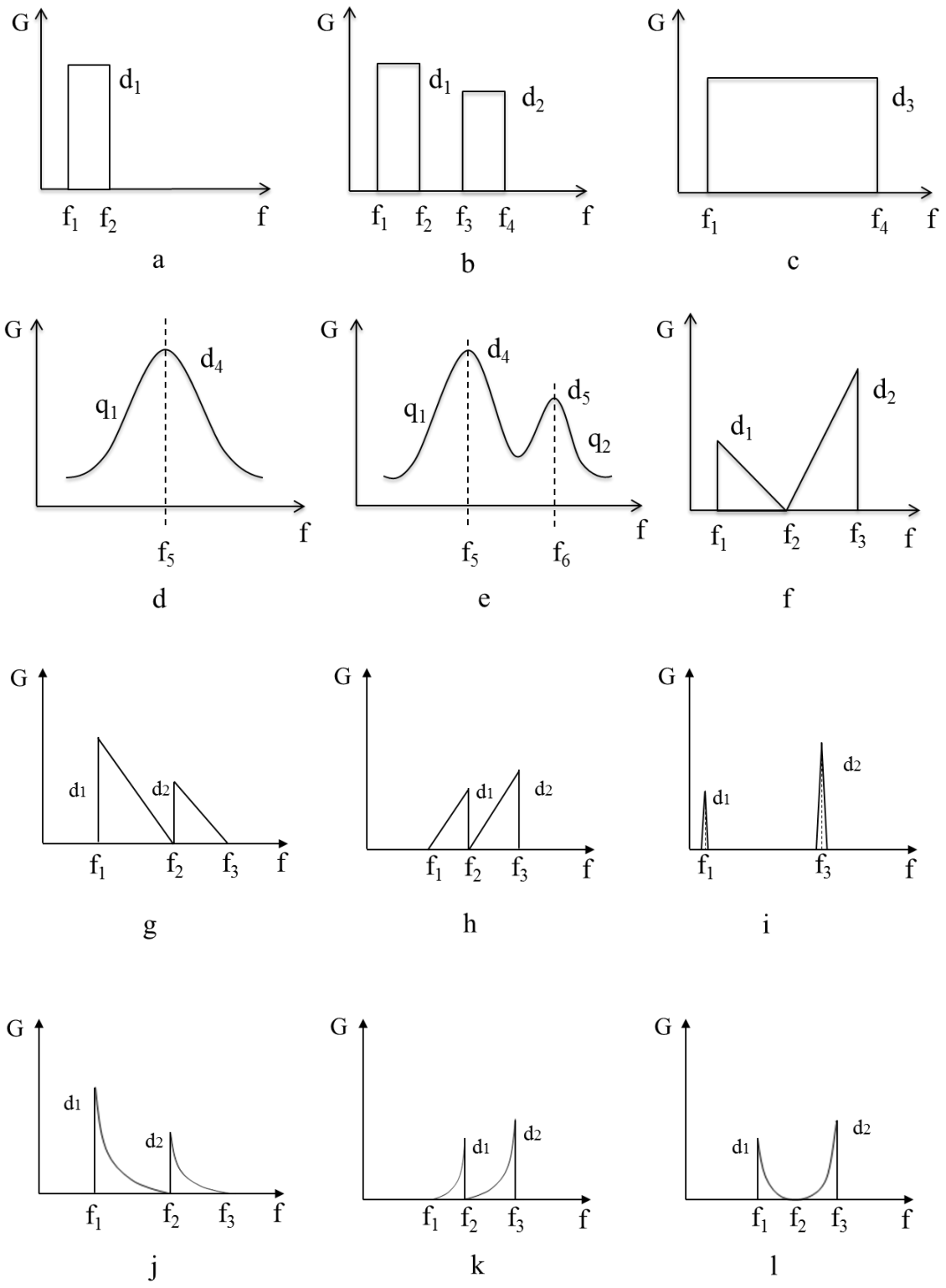
G
d1
f1 f2 f
a
G
d1
d2
f1 f2 f3 f4 f
b
G
d3
f1 f4 f
c
G
d4
q1
f
f5
d
G
d4
q1
d5
q2
f
f5 f6
e
G
d2
d1
f1 f2 f3 f
f
G
d1
d2
f1 f2 f3 f
g
G
d1
d2
f1 f2 f3 f
h
G
d2
d1
f1 f3 f
i
G
d1
d2
f1 f2 f3 f
j
G
d1
d2
f1 f2 f3 f
k
G
d2
d1
f1 f2 f3 f
l

Figure 1

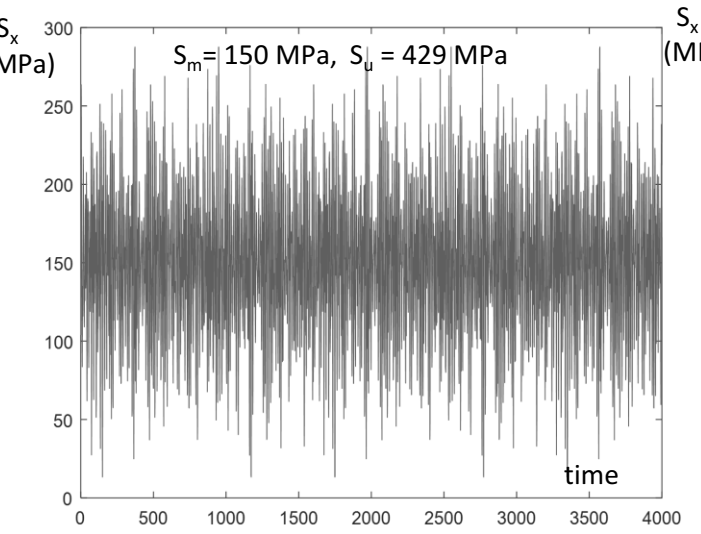

(a)

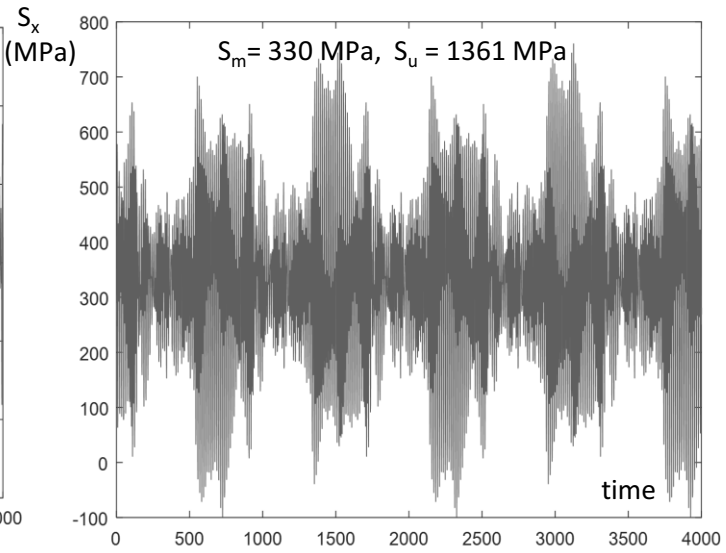

(b)

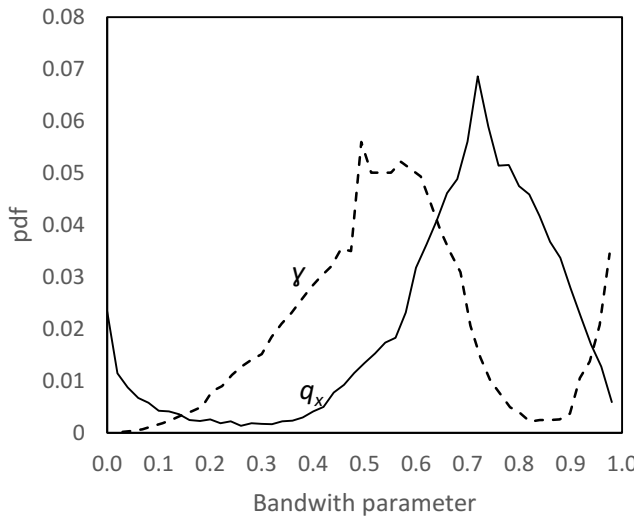

(c)

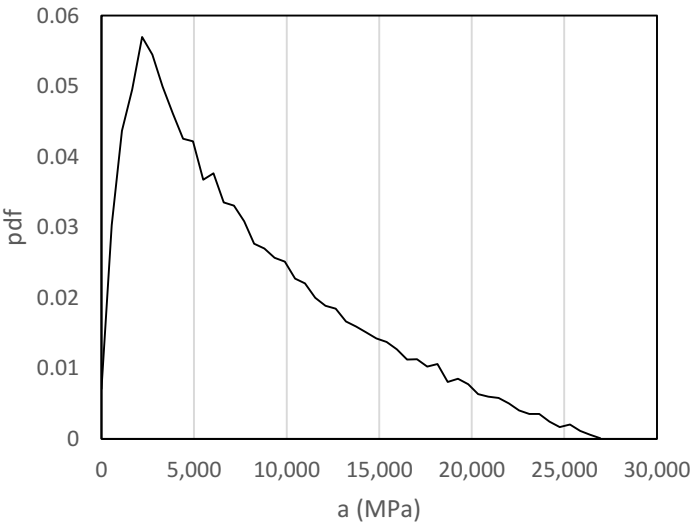

(d)

Figure 2

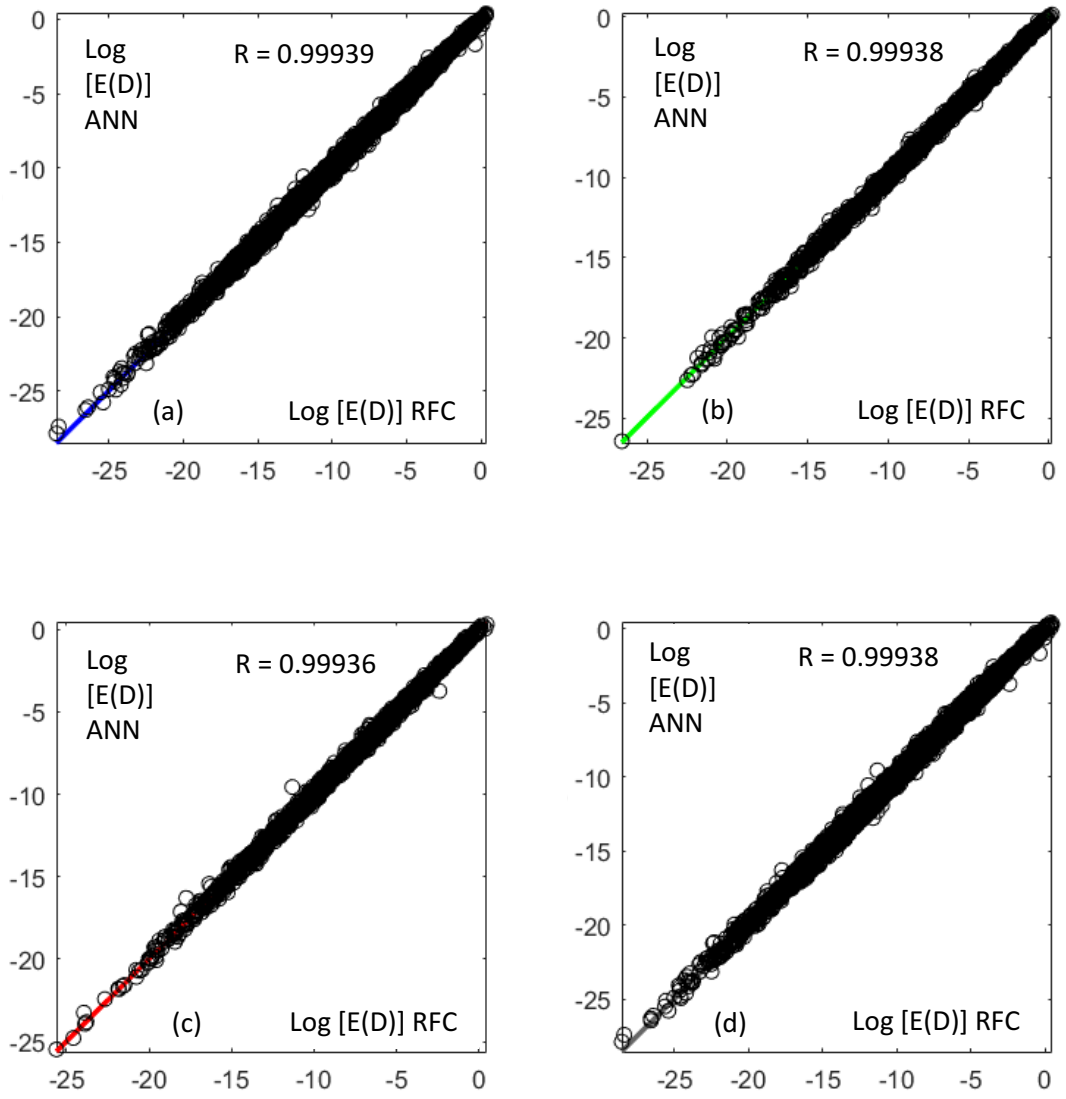
Log
[E(D)]
ANN
R = 0.99939
(a)
Log [E(D)] RFC
Log
[E(D)]
ANN
R = 0.99938
(b)
Log [E(D)] RFC
Log
[E(D)]
ANN
R = 0.99936
(c)
Log [E(D)] RFC
Log
[E(D)]
ANN
R = 0.99938
(d)
Log [E(D)] RFC

Figure 3

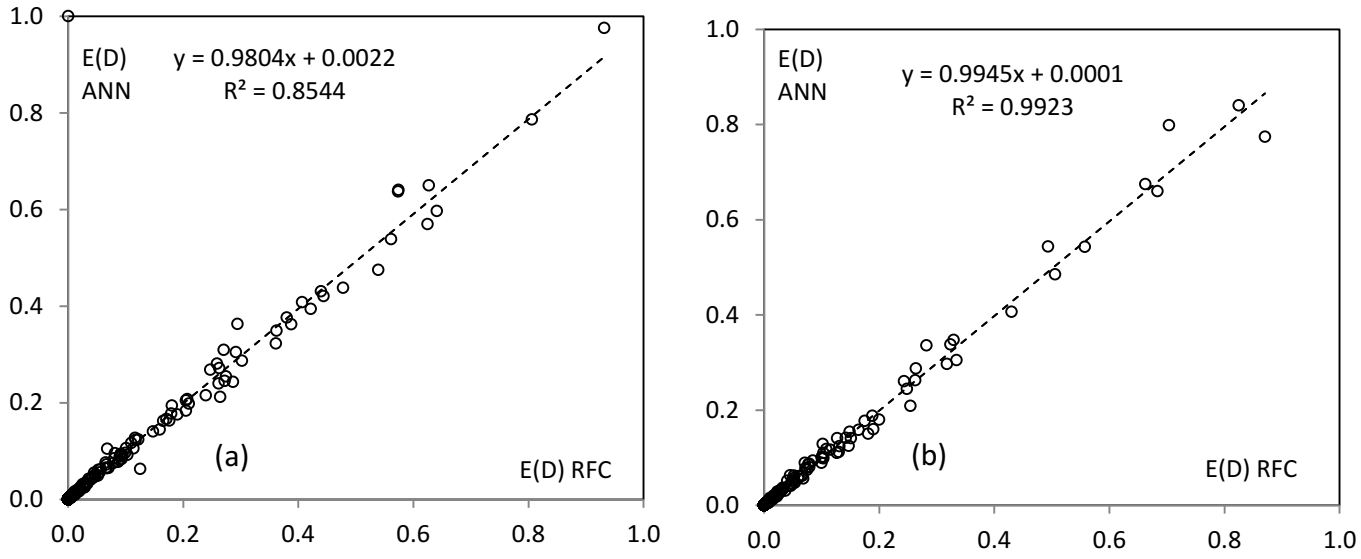
E(D) ANN
y = 0.9804x + 0.0022
R² = 0.8544
(a)
E(D) RFC
E(D) ANN
y = 0.9945x + 0.0001
R² = 0.9923
(b)
E(D) RFC

Figure 4

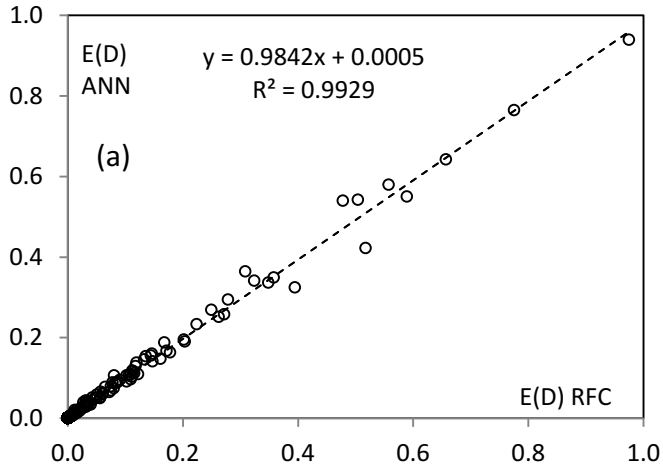

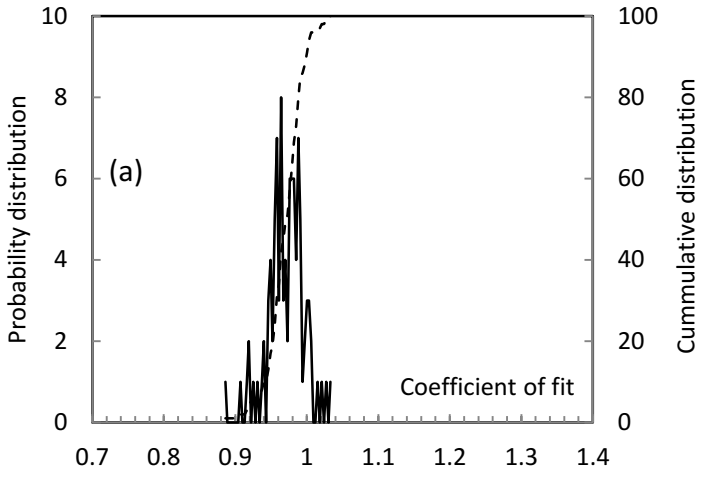

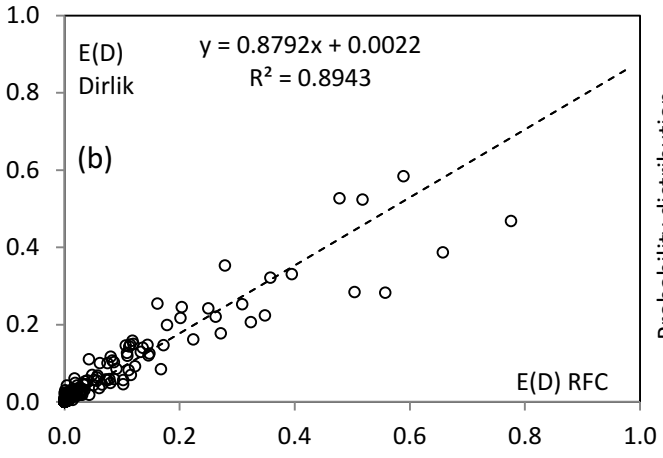

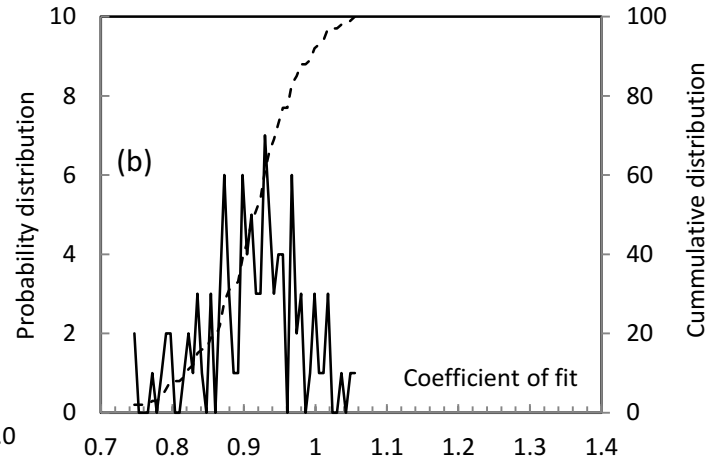

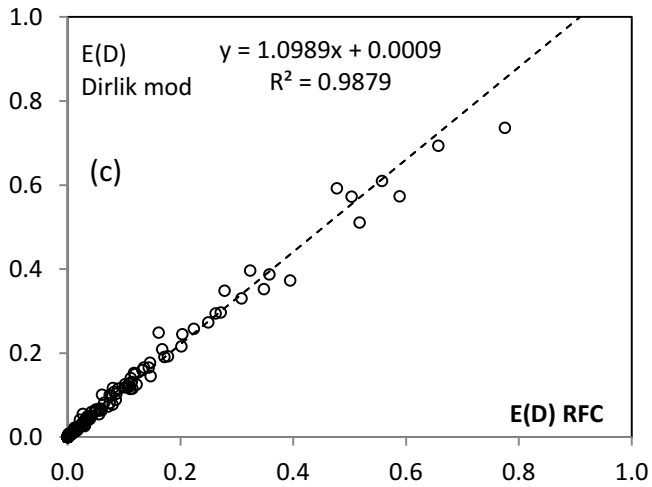

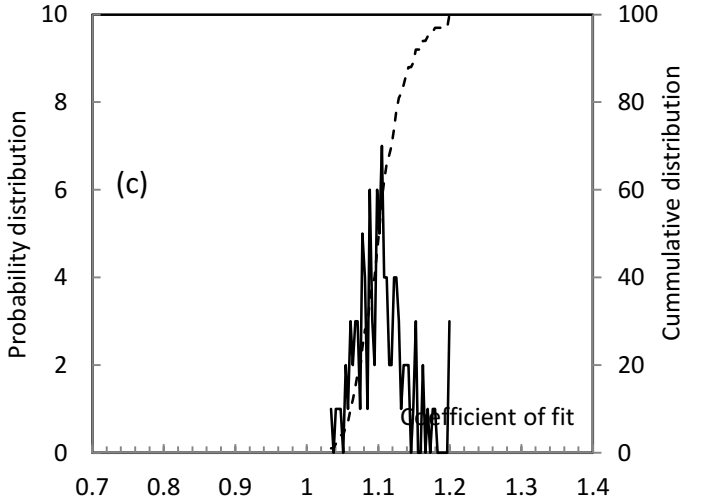

Figure 5

Figure 6

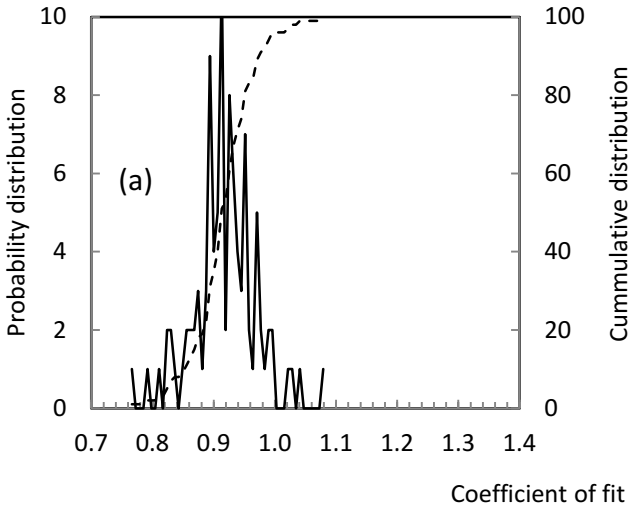

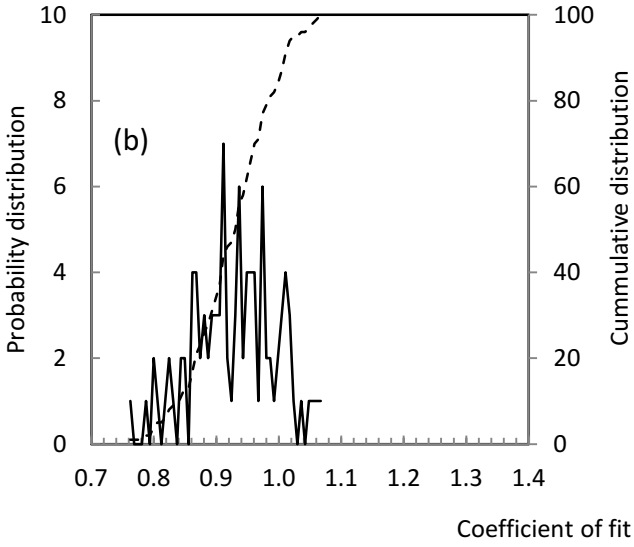

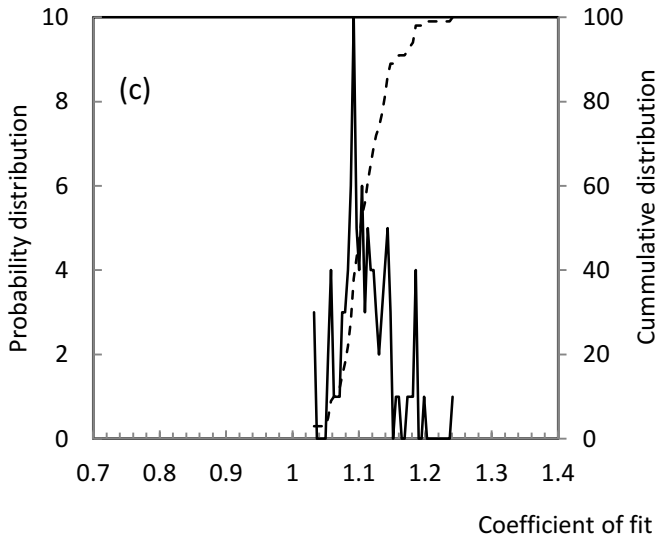

Figure 7

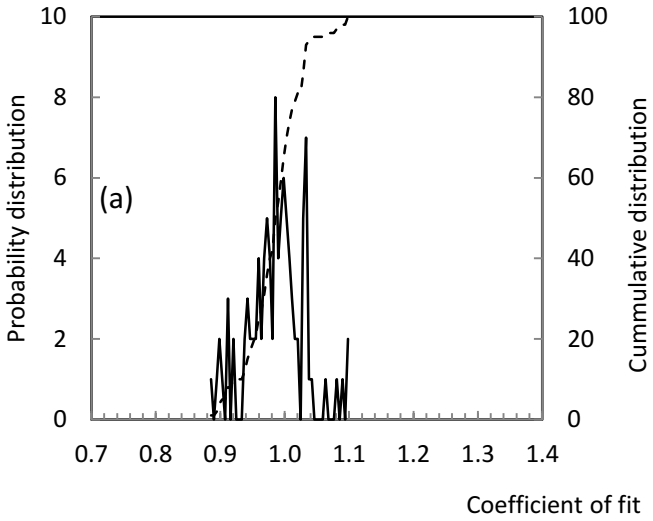

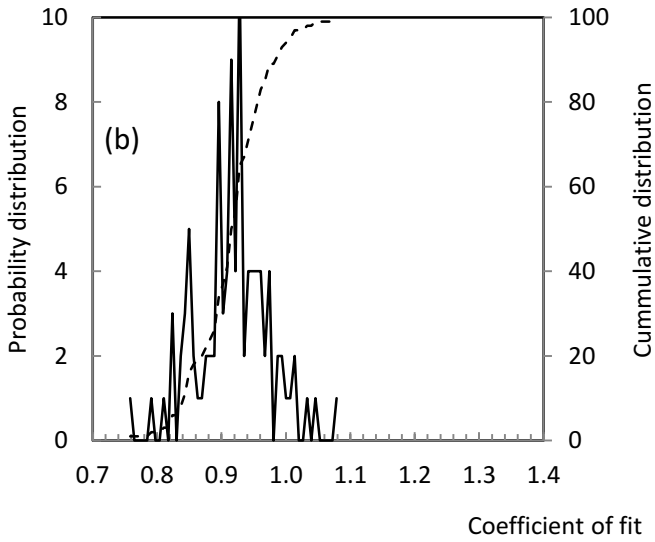

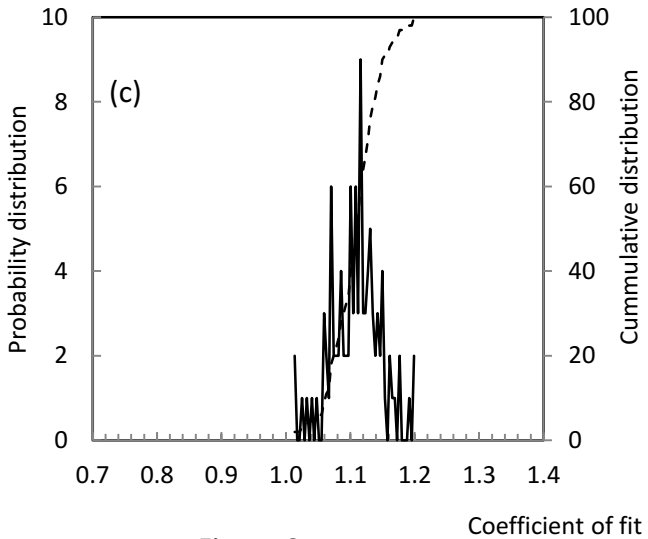

Figure 8

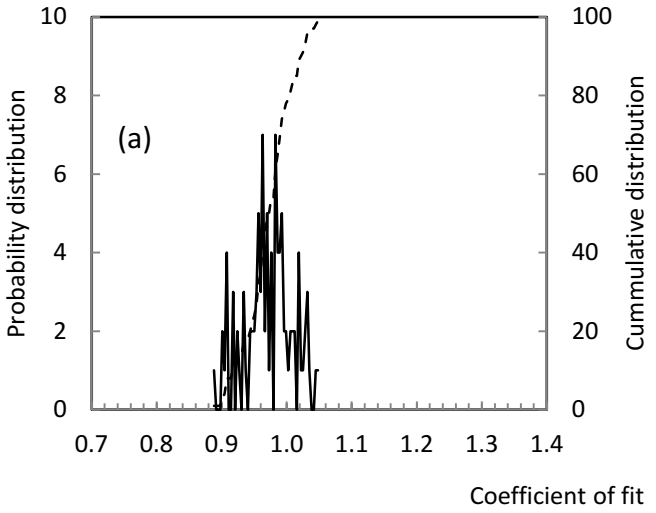

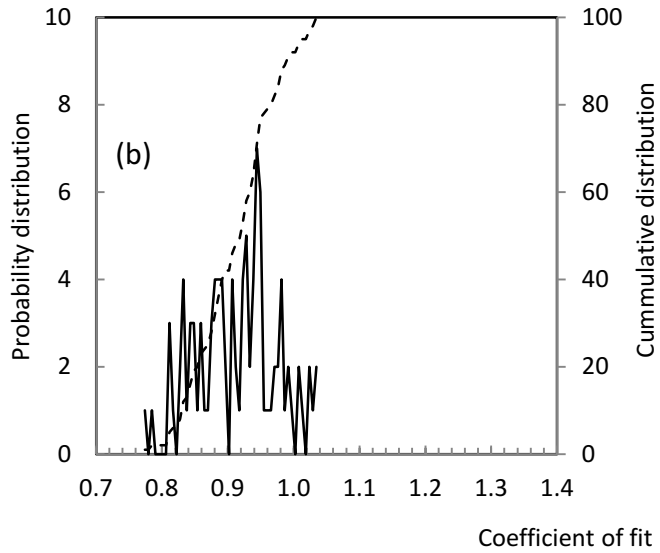

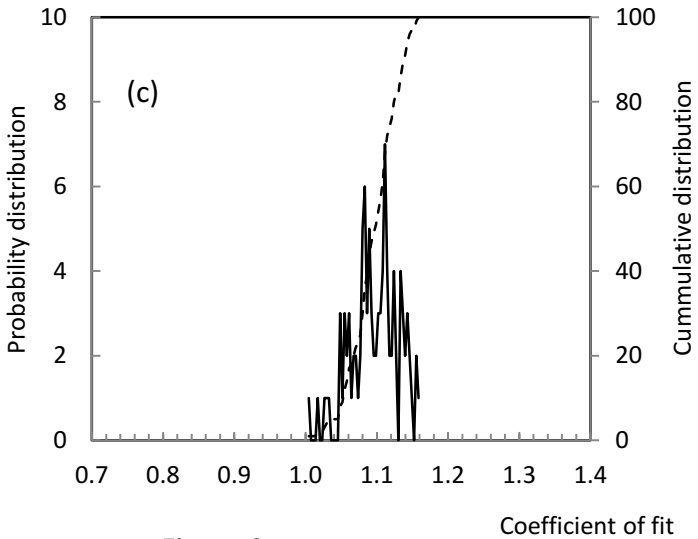

Figure 9

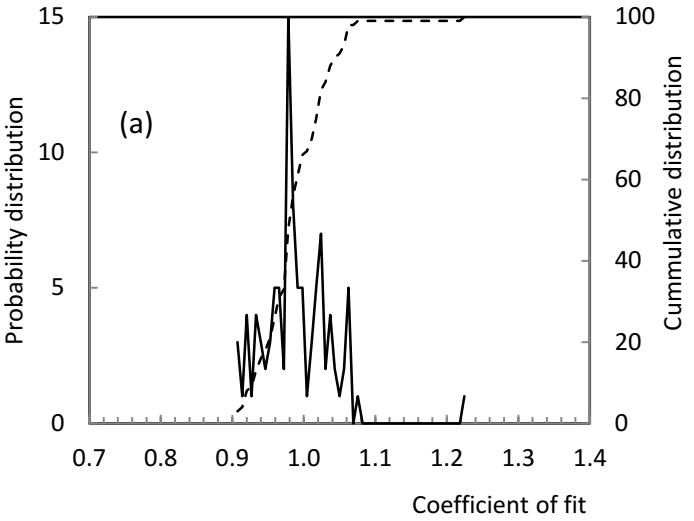

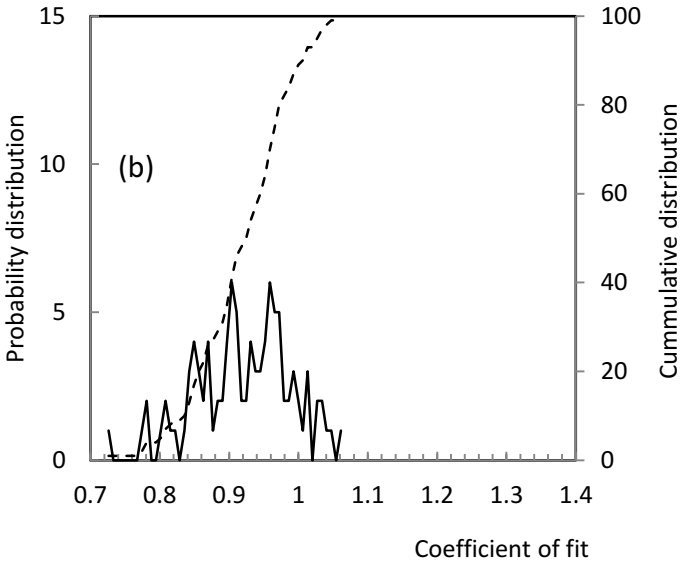

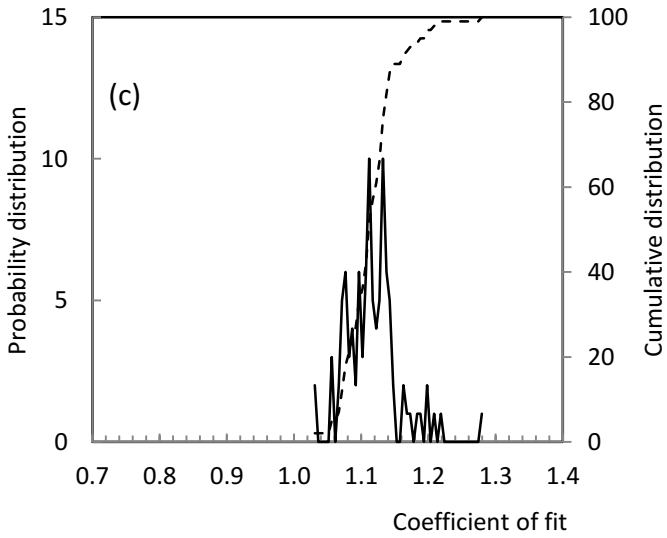

Figure 10

ANN type	No of inputs	Input	output
ANN1	7	$m_0, m_1, m_2, m_4, a, b, S_u$	Log[E(D)]
ANN2	8	$m_0, m_1, m_2, m_4, a, b, S_u, \alpha_m$	
ANN3	9	$m_0, m_1, m_2, m_4, a, b, S_u, \alpha_m, \alpha_c,$	
ANN4	11	$m_0, m_1, m_2, m_4, a, b, S_u, \alpha_m, \alpha_c, \gamma_p, \gamma_n$	
ANN5	8	$m_{o0}, m_{01}, m_{02}, m_{o4}, a, b, S_u, K_G$	

Table 1

Prop	S_u(MPa)	a (MPa)	b	m_0	m_1	m_2	m_4
Min	200	261	-0.333	1.86E+01	6.71E+02	1.49E+04	2.85E+06
Max	2000	26543	-0.085	4.13E+05	3.89E+07	5.27E+09	1.07E+14

Table 2

Signal	RFC	ANN4	Signal	RFC	ANN4
1	-1.6235	-1.6273	11	-0.5320	-0.5546
2	-4.2077	-4.1976	12	-4.3904	-4.4466
3	-1.2419	-1.2246	13	-1.2854	-1.3617
4	-3.4617	-3.4271	14	-2.0673	-2.0033
5	-2.9667	-2.9542	15	-2.8691	-2.8299
6	-4.8385	-5.0301	16	-2.1123	-2.0044
7	-3.6356	-3.5645	17	-1.0356	-1.0150
8	-2.7532	-2.7815	18	-2.0217	-1.9996
9	-5.3277	-5.1328	19	-3.4093	-3.5487
10	-3.5928	-3.6411	20	-4.1959	-3.7849

(a)

Signal	RFC	ANN4	Signal	RFC	ANN4
1	-1.3476	-1.3517	11	-1.3832	-1.4041
2	-3.0961	-3.0989	12	-3.6364	-3.6554
3	-4.9092	-4.9056	13	-4.2279	-4.1279
4	-3.9604	-3.8810	14	-1.8428	-1.8204
5	-3.9281	-3.9611	15	-2.3793	-2.4285
6	-2.4174	-2.5214	16	-1.6329	-1.6657
7	-1.9736	-1.9532	17	-4.7976	-4.7679
8	-0.4431	-0.4798	18	-2.6371	-2.6608
9	-4.1736	-4.2710	19	-2.2660	-2.2759
10	-1.3544	-1.3911	20	-3.5004	-3.5154

(b)

Table 3

Signal	RFC	ANN4	Dirlik	Dirlik(M)
1	-3.7915	-3.7785	-3.6619	-3.6931
2	-3.7202	-3.6828	-3.7382	-3.5634
3	-1.6697	-1.6793	-1.5527	-1.5836
4	-4.3951	-4.4030	-4.3156	-4.1834
5	-2.4100	-2.3833	-1.3760	-2.3865
6	-1.2419	-1.1878	-1.1647	-1.1661
7	-5.0037	-4.8730	-4.4391	-4.5923
8	-5.1035	-5.0605	-4.8552	-4.9499
9	-4.4168	-4.3236	-3.0497	-4.2218
10	-3.2446	-3.2332	-3.0723	-2.8670

(a)

Signal	RFC	ANN4	Dirlik	Dirlik(M)
1	-5.1683	-5.1402	-3.7306	-5.9750
2	-3.3922	-3.4292	-2.8478	-3.2523
3	-2.7254	-2.6775	-2.6843	-2.6212
4	-5.3526	-5.6698	-5.1473	-5.1473
5	-2.2710	-2.3523	-2.1428	-2.1597
6	-1.5106	-1.3653	-1.7361	-1.3976
7	-5.1224	-5.0853	-2.2117	-4.9353
8	-5.3422	-5.3669	-4.2380	-5.1366
9	-5.9307	-5.9963	-5.8906	-5.8596
10	-3.6099	-3.5784	-3.4930	-3.4510

(b)

Table 4

Batch	Coefficient of fit			RMS error		
	ANN4	Dirlik	Dirlik(M)	ANN4	Dirlik	Dirlik(M)
1	0.9891	0.9093	1.0882	0.0004	0.0023	0.0011
2	0.9622	0.7992	1.1083	0.0009	0.0036	0.0010
3	0.9448	0.9646	1.0435	0.0008	0.0017	0.0019
4	0.9778	0.9683	1.0975	0.0006	0.0015	0.0010
5	0.9807	0.9361	1.0975	0.0003	0.0012	0.0006
6	0.9567	1.0046	1.1393	0.0009	0.0007	0.0004
7	1.0149	0.9550	1.1352	-0.0001	0.0013	0.0001
8	0.9633	0.8967	1.0534	0.0005	0.0012	0.0016
9	0.9776	0.9297	1.0977	0.0005	0.0018	0.0008
10	0.9199	0.7937	1.0473	0.0014	0.0046	0.0020
Mean	**0.9687**	**0.9157**	**1.0908**	**0.0006**	**0.0020**	**0.0011**
Std	**0.0259**	**0.0700**	**0.0338**	**0.0004**	**0.0012**	**0.0006**

(a)

Batch	Coefficient of fit			RMS error		
	ANN4	Dirlik	Dirlik(M)	ANN4	Dirlik	Dirlik(M)
1	0.9650	0.8805	1.0676	0.0115	0.0162	0.0121
2	0.9744	0.9422	1.0765	0.0098	0.0166	0.0112
3	0.9911	0.9456	1.1409	0.0132	0.0273	0.0225
4	0.9734	0.9377	1.0980	0.0100	0.0148	0.0135
5	0.9778	0.9147	1.0998	0.0092	0.0159	0.0143
6	0.9876	0.9061	1.1226	0.0149	0.0231	0.0223
7	0.9571	0.8226	1.0611	0.0121	0.0150	0.0139
8	0.9773	0.8772	1.1309	0.0133	0.0309	0.0283
9	0.9609	0.8447	1.1105	0.0099	0.0185	0.0147
10	0.9607	0.8935	1.1107	0.0112	0.0161	0.0146
Mean	**0.9725**	**0.8965**	**1.1018**	**0.0115**	**0.0194**	**0.0167**
Std	**0.0115**	**0.0414**	**0.0268**	**0.0019**	**0.0057**	**0.0056**

Table 5 (b)

Signals	ANN4	Dirlik	Dirlik(M)	ANN4	Dirlik	Dirlik(M)
500	1.1582	0.9478	1.1224	0.0663	0.0198	0.0174
1000	0.9506	0.9220	1.0937	0.0182	0.0207	0.0174
2000	1.0425	0.9409	1.1150	0.0242	0.0190	0.0172
5000	1.0005	0.9272	1.1103	0.0145	0.0196	0.0166
10000	0.9758	0.8933	1.0943	0.0108	0.0164	0.0143
20000	0.9661	0.8942	1.0841	0.0112	0.0171	0.0153
50000	0.9729	0.9261	1.1030	0.0117	0.0193	0.0173

(a)

Signals	ANN4	Dirlik	Dirlik(M)	ANN4	Dirlik	Dirlik(M)
500	0.2024	0.0267	0.0327	0.0451	0.0051	0.0039
1000	0.0358	0.0523	0.0356	0.0044	0.0073	0.0037
2000	0.0419	0.0644	0.0262	0.0099	0.0041	0.0042
5000	0.0265	0.0412	0.0276	0.0024	0.0030	0.0031
10000	0.0287	0.0747	0.0322	0.0032	0.0035	0.0025
20000	0.0220	0.0747	0.0392	0.0024	0.0047	0.0041
50000	0.0272	0.0788	0.0404	0.0046	0.0036	0.0041

(b)

Table 3